# Solar Gamma-Ray Physics Comes of Age

Gerald H. Share and Ronald J. Murphy

*E.O. Hulburt Center for Space Research*
*Naval Research Laboratory, Washington D.C., 20375*

**Abstract.** The launch of NASA's *HESSI* satellite will provide solar scientists with ≥ 2arcsec imaging/≥ 2 keV spectroscopy of solar flares from ~10 keV to 10 MeV for the first time. We summarize recent developments in our understanding of solar flares based primarily on gamma-ray line measurements made over the past twenty years with instruments having moderate spectral resolution. These measurements have provided information on solar ambient abundance, density and temperature; accelerated particle composition, spectra, and transport; and flare energetics.

## RELATIONSHIP TO CELESTIAL GAMMA RADIATION

This conference primarily focuses on gamma rays from galactic and extra-galactic sources. These sources produce radiation that has been measured up to TeV energies [1] and is primarily in the form of continuum emission from relativistic electrons. Gamma-ray lines have been detected only from de-excitations of freshly produced radioactive nuclei in supernovae [2] and in relic radiation from earlier explosions [3,4]. To date there have been no observations of celestial gamma-ray lines from nuclei excited by collisions with energetic ions [5]. The most likely source of these lines is cosmic-ray proton interactions with the interstellar medium [6]. Interactions of higher-energy protons create pions that decay and produce a characteristic broad feature near 70 MeV that has been detected from the Galactic plane [7]. High-energy bremsstrahlung from relativistic electrons can mask the presence of this feature, however [8].

## GAMMA-RAY PRODUCTION DURING SOLAR FLARES

The sun is a prolific source of high-energy electrons, ions, and neutrons during solar flares. These flares can produce particles with energies up to tens of GeV that are revealed by ground-based measurements [9] and gamma-ray observations in space [10]. The primary source for particle acceleration is the energy contained in the sun's magnetic field. How this conversion of magnetic energy to kinetic energy takes place is still not known, however, reconnection is a likely mechanism [11].

We show a simple representation of this process in Figure 1. The image in the upper left corner was taken during a limb flare by the Yohkoh satellite [12]. The contours show the hard X-ray sources and the gray scale shows the image in soft X rays. The full magnetic loop filled with hot plasma is revealed in soft X-rays. In

# Report Documentation Page

*Form Approved*
*OMB No. 0704-0188*



| 1. REPORT DATE | 2. REPORT TYPE | 3. DATES COVERED |
|---|---|---|
| **2001** | | **00-00-2001 to 00-00-2001** |

| 4. TITLE AND SUBTITLE | 5a. CONTRACT NUMBER |
|---|---|
| **Solar Gamma-Ray Physics Comes of Age** | 5b. GRANT NUMBER |
| | 5c. PROGRAM ELEMENT NUMBER |
| 6. AUTHOR(S) | 5d. PROJECT NUMBER |
| | 5e. TASK NUMBER |
| | 5f. WORK UNIT NUMBER |
| 7. PERFORMING ORGANIZATION NAME(S) AND ADDRESS(ES) **Naval Research Laboratory,E. O. Hulburt Center for Space Research,4555 Overlook Avenue, SW,Washington,DC,20375** | 8. PERFORMING ORGANIZATION REPORT NUMBER |
| 9. SPONSORING/MONITORING AGENCY NAME(S) AND ADDRESS(ES) | 10. SPONSOR/MONITOR'S ACRONYM(S) |
| | 11. SPONSOR/MONITOR'S REPORT NUMBER(S) |

12. DISTRIBUTION/AVAILABILITY STATEMENT
**Approved for public release; distribution unlimited**

13. SUPPLEMENTARY NOTES
**AIP Conference Proceedings, 587, 603 (2001).**

14. ABSTRACT
**The launch of NASA?s HESSI satellite will provide solar scientists with ≥ 2arcsec imaging/≥ 2 keV spectroscopy of solar flares from ~10 keV to 10 MeV for the first time. We summarize recent developments in our understanding of solar flares based primarily on gammaray line measurements made over the past twenty years with instruments having moderate spectral resolution. These measurements have provided information on solar ambient abundance, density and temperature; accelerated particle composition, spectra, and transport and flare energetics.**

15. SUBJECT TERMS

| 16. SECURITY CLASSIFICATION OF: | | | 17. LIMITATION OF ABSTRACT | 18. NUMBER OF PAGES | 19a. NAME OF RESPONSIBLE PERSON |
|---|---|---|---|---|---|
| a. REPORT | b. ABSTRACT | c. THIS PAGE | | | |
| **unclassified** | **unclassified** | **unclassified** | **Same as Report (SAR)** | **10** | |

contrast the hard X rays reveal the footpoints of the loops where the accelerated particles interact. A hard X ray source also appears above the soft X-ray loop. This region may represent the location where the energy for the flare originates although particle acceleration may occur all along the loop structure [11]. The hard X-ray intensities from the foot points are often different from one another and have an inverse relationship with microwave emissions. This suggests that the electrons have a higher probability of impacting the solar atmosphere where the magnetic field is weaker.

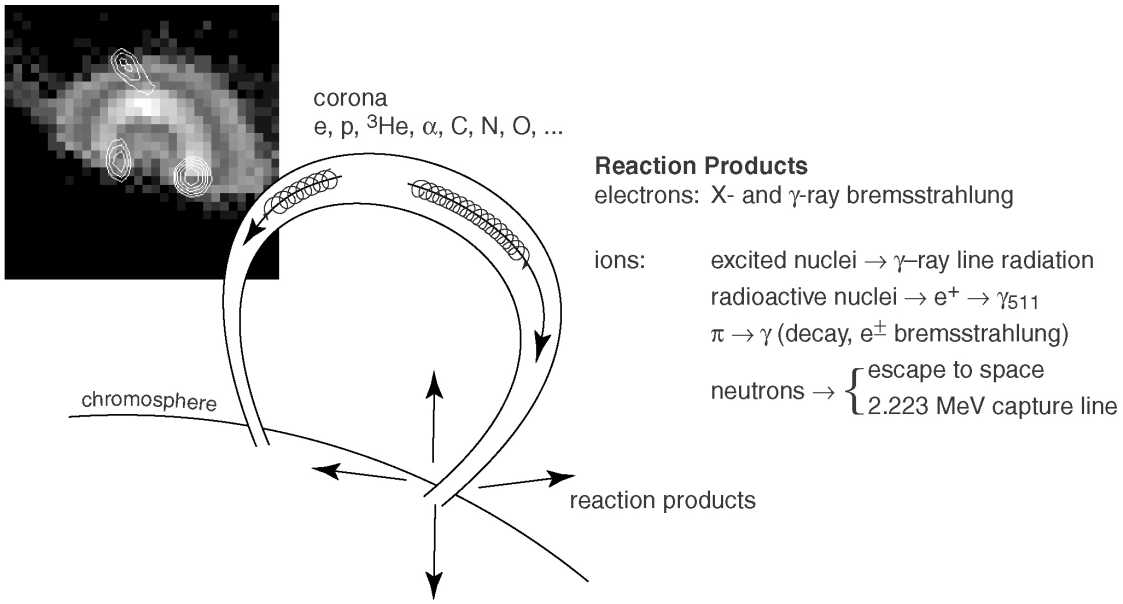


**FIGURE 1.** Schematic showing particle acceleration and interaction in magnetic loops during solar flares.

With the upcoming launch of the *HESSI* satellite that offers the promise of high-resolution spectroscopy of solar flares [13], we shall focus our remarks primarily on what has been learned from γ-ray line spectroscopy. Figure 2 shows the γ-ray spectrum of the 1991 June 4 X12+ solar flare (N30E70) observed by the *Compton Gamma Ray Observatory (CGRO)* OSSE experiment [14]. The captions describe how γ-ray line and continuum studies reveal the physics of flares [6,15-19]. We use this figure to illustrate what has been learned about ion acceleration, transport, and interaction in flares. The spectrum covers the range from 100 keV to 10 MeV and exhibits an electron bremsstrahlung continuum that has a power-law shape extending to high energies. The continuum doesn't always follow a single power law. It often steepens or hardens above a few hundred keV, and sometimes further hardens ≥ 1 MeV [20]. Nuclear lines are superposed above the power law continuum. These include lines from de-excitation of directly excited nuclei and spallation products in the solar atmosphere after impact by flare-accelerated protons and α particles. De-excitation lines from Mg, Si, Fe, Ne, C and O referred to in the figure are broadened by ~1-2% by nuclear recoil. The spectrum also contains very broad lines produced

when flare-accelerated heavy nuclei impact atmospheric H and He. Two other prominent line features appear in the spectrum at 0.511 MeV and 2.223 MeV. These lines originate from positron-electron annihilation and neutron capture on H, respectively. Below we discuss our current understanding of the characteristics of nuclear lines and their relationship to the physics of solar flares.

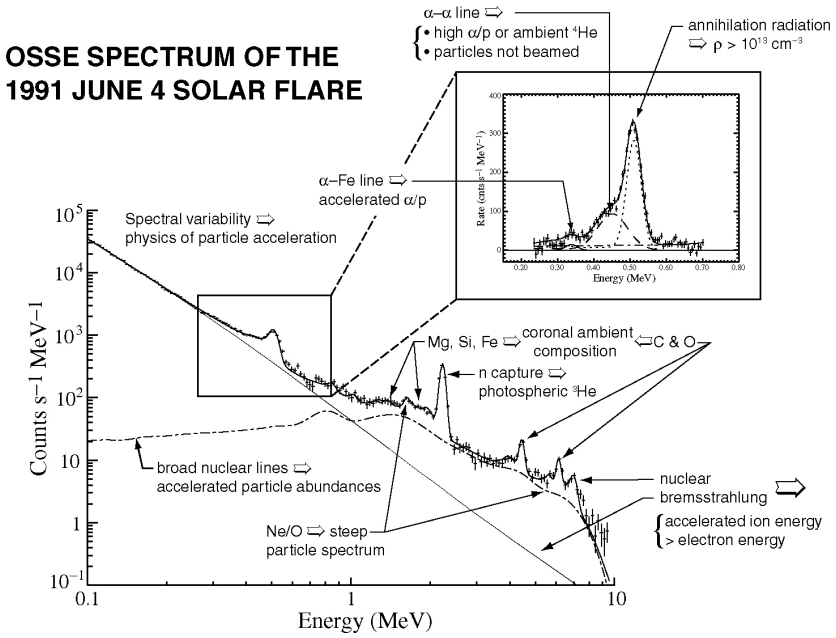


**FIGURE 2.** OSSE spectrum of the 1991 June 4 solar flare summarizing the physics revealed by γ-ray spectroscopy.

## Narrow Gamma-Ray Line Studies

About 30% of all flares with emission >0.3 MeV exhibit clear evidence for nuclear lines. This evidence is usually provided by detection of the neutron capture line at 2.223 MeV or other strong narrow lines. The presence of a nuclear component may also be revealed by general characteristics of the spectrum such as hardening above ~1 MeV and steepening >7 MeV, where few nuclear lines are produced. Additional studies based on these characteristics indicate that an even higher percentage of high-energy flares have a nuclear component [21] (see also Young, *et al.* in these proceedings). Narrow γ-ray line observations are key to understanding the characteristics of accelerated protons and α particles at the Sun. They also provide information on ambient composition, temperature, and density of the flare plasma [6,15,19,20].

## *Hydrogen Neutron-Capture Line*

The 2.223 MeV neutron-capture line is the most prominent line observed in spectra of flares that are not too close to the limb (see Figure 2). Because it is produced by capture of neutrons after they slow down deep in the solar atmosphere, the line is narrow, delayed in time, and significantly attenuated for flares near the limb. The line's narrow width and strength makes it an excellent indicator of the presence of ions in flares. It therefore has been used to search for a threshold in ion acceleration using combined data from *SMM*/GRS and *CGRO*/OSSE [22] and for continuous acceleration of ions during solar quiet times [23,24]. Measurement of its intensity and temporal variation relative to prompt de-excitation lines has provided information on the spectra of ions above ~10 MeV and on the concentration of $^3$He in the photosphere [25]. The latter measurements are possible because $^3$He nuclei capture neutrons in competition with photospheric hydrogen and therefore affect the decay time of the 2.223 MeV capture line. Observations with *SMM*, *GRANAT*, *CGRO* and *Yohkoh* suggest photospheric $^3$He/H ratios of ~ 2 - 4 x $10^{-5}$ [26]. These ratios are dependent on assumptions concerning the depth of interaction and solar atmospheric model, however.

## *Positron-Electron Annihilation Line*

Positrons from decay of radioactive nuclei and high-energy pions annihilate with electrons to produce the 0.511 MeV line. Comparison of its intensity profile with those from de-excitation lines provides information on both the species of radioactive nuclei and the density of the medium where the positrons annihilate [15]. It is also an excellent diagnostic for flares that exhibit a distinct second stage during which the proton spectrum is hard enough to produce pions. A classic example is the 1991 July 11 flare observed by the EGRET, COMPTEL, and OSSE instruments on *CGRO* [10]. The annihilation line peaks in coincidence with the high-energy emission suggesting a $\pi^+$ origin [27].

Measurements of the 0.511 MeV line width and positronium continuum provide information about the temperature and density of the ambient material. The inset of Figure 1 shows the region of the annihilation line observed by OSSE. Detailed measurements of the line and continuum have been made in seven flares using the moderate resolution spectrometer on *SMM* [28]. We plot the measured $3\gamma/2\gamma$ ratio vs. line width in Figure 3; the curve shows the results of a calculation. The positronium continuum/line ratio in the flares are all significantly lower than that measured by *SMM* for the Galactic plane emission; these low ratios indicate temperatures $>10^5$ K in the flare plasma. The width of the annihilation line becomes broad enough to be resolved by *SMM* for temperatures $>10^6$ K; the line in flare '14' appears to have been formed at such high temperatures. There is also one flare, '9', for which the $3\gamma/2\gamma$ ratio falls significantly below the curve; this suggests a local density $>10^{14}$ cm$^{-3}$.

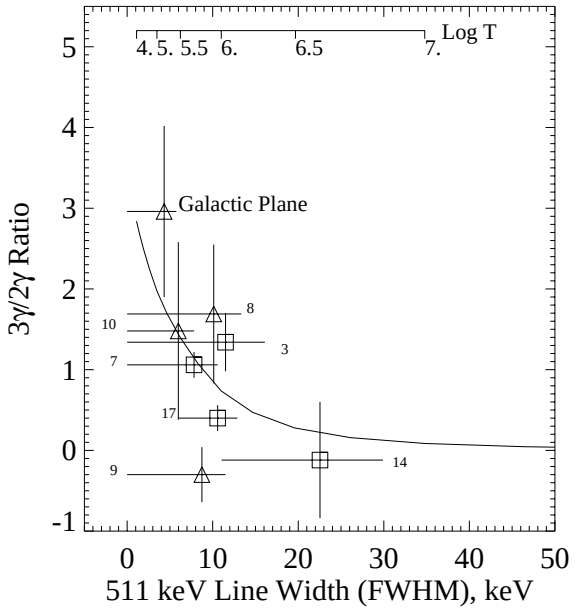


**FIGURE 3.** *SMM* measurements of the 3γ/2γ positron annihilation ratio compared with the 511 keV line width for 7 flares.

## *Narrow De-excitation Lines*

To date about 18 relatively narrow de-excitation lines have been identified in solar flares: $^{59}$Ni (0.339 MeV), $^{7}$Be (0.429), $^{7}$Li (0.478), $^{56}$Fe (0.847), $^{18}$F (0.937), $^{18}$F/$^{58}$Co/$^{58}$Ni/$^{59}$Ni (1.00-1.08), $^{56}$Fe (1.238), $^{55}$Fe (1.317), $^{24}$Mg (1.369), $^{20}$Ne (1.633), $^{28}$Si (1.779), $^{32}$S /$^{14}$N (2.230/2.313), $^{20}$Ne (3.334), $^{12}$C (4.439), $^{15}$N/$^{15}$N/$^{15}$O (~5.3), $^{16}$O (6.130), $^{11}$C (6.337, 6.476), $^{14}$N/$^{16}$O (7.028/6.919). These lines were identified from the summed spectrum of 19 intense flares observed by the *SMM* spectrometer [28, 29] that we plot in Figure 4.

Our fits to some of the prominent de-excitation lines, e.g. $^{12}$C, in this summed spectrum indicated widths that were about a factor of two larger than expected [6, 20]. We therefore studied whether this increase could be due to changes in the line energies from flare to flare. Not only was this true, but we also found that the fitted energy was dependent on the flare's heliocentric angle. We show this variation in Figure 5 where we plot the fitted energies of the $^{12}$C, $^{16}$O, $^{20}$Ne de-excitation lines in flares grouped according to the cosine of heliocentric angle. The lines are Doppler-shifted by ~1% for flares near the center of the solar disk. Note that there is no significant redshift for the 2.223 MeV neutron capture line, which is formed at rest (other higher energy lines contribute near the limb where the line is weak). This is the first evidence for such a redshift in nuclear lines during flares and indicates that accelerated ions preferentially interact in a downward direction.

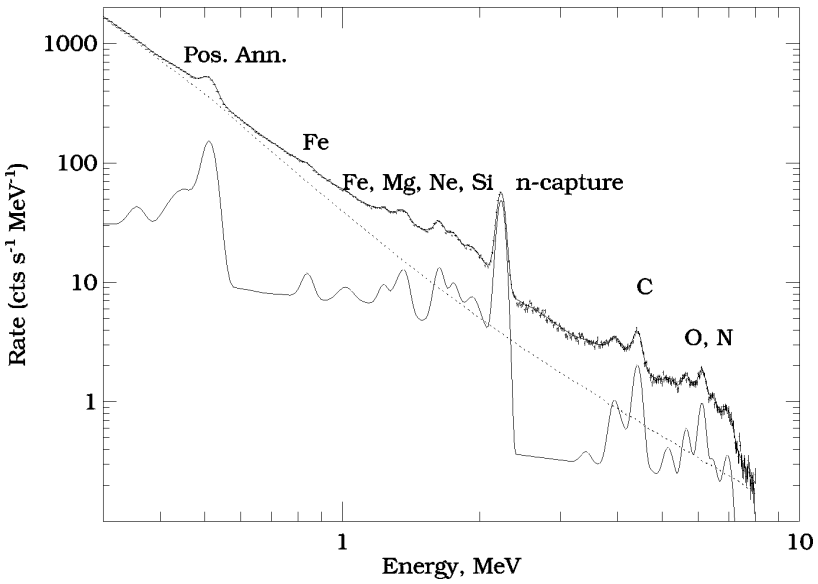


**FIGURE 4.** Count spectrum derived from the sum of 19 flares observed by *SMM*. Solid curve drawn through the points is best fit. The thin curve shows the best fit to the narrow lines.

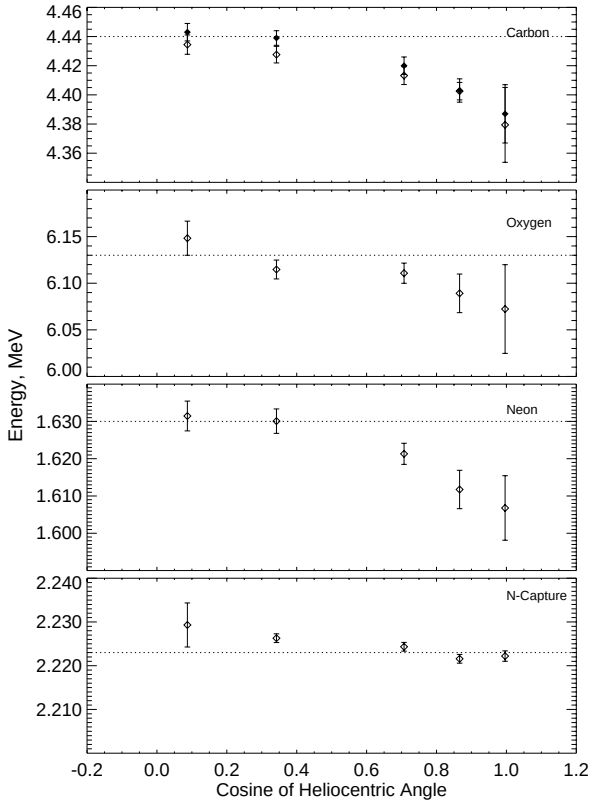


**FIGURE 5.** Variation of narrow de-excitation line energies with respect to heliocentric angle of the flare.

We found flare-to-flare variations in relative line fluences in the 19 solar flares [29], suggesting that the abundances of elements in the plasma group with respect to first ionization potential (FIP). Using these published line fluences, measured cross sections, and kinematical calculations, Ramaty, *et al.* [30] showed that the composition of the flare plasma is, on average, close to coronal. This is illustrated in Figure 6 where they compare the observed $^{24}$Mg (low FIP)/$^{16}$O (high FIP) line ratios. A photospheric ambient abundance would require extremely steep accelerated particle spectra that are inconsistent with observations for most of the flares. However, flare '9' appears depleted in low FIP emission lines; this suggests a composition closer to that of the photosphere. As discussed in the section on positron annihilation above, there is other evidence for believing that the $\gamma$ rays from this flare may have been produced at depths where the ambient composition was closer to photospheric. This suggests that flare particles may interact in plasmas with compositions ranging from those found in the upper photosphere to those in the corona. Recently reported spectroscopic measurements of flares with OSSE [14] suggest that the ambient composition may also change within flares. This implies that ions accelerated in different flares and at different times in flares may interact at significantly different depths in the solar atmosphere. This could happen, for example, if the height of magnetic mirroring increases with time.

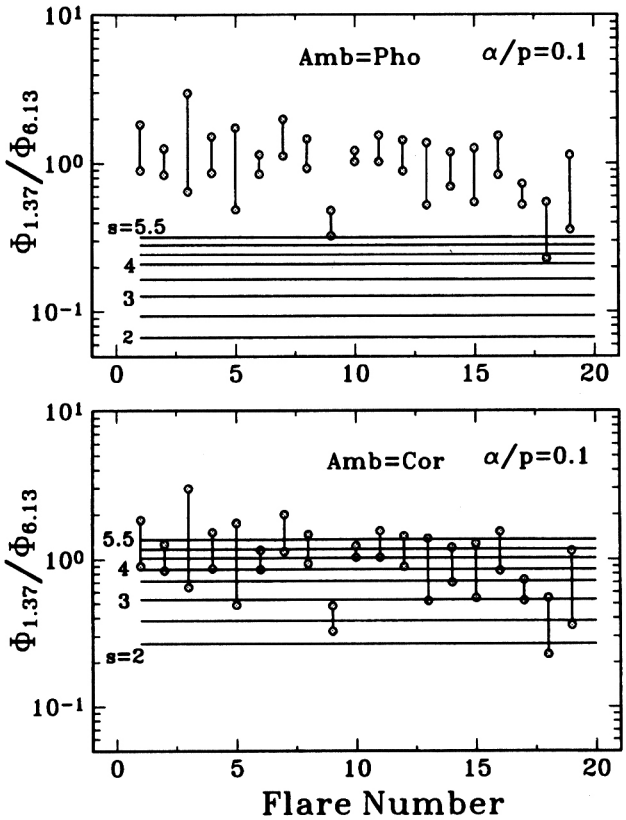


**FIGURE 6.** Measured Mg/O line ratios for 19 flares compared with calculations for photospheric and coronal ambient composition [30].

Another narrow line ratio, $^{20}Ne/^{16}O$, can be used to estimate the spectrum of accelerated ions above ~5 MeV [29]. The measurements are consistent with power laws [30]. Assuming that these power laws extend down to 1 MeV, Ramaty and Mandzhavidze [19] compared the energies contained in accelerated ions and electrons (>20 keV). We show this comparison in Figure 7 for the 19 SMM flares and also for the 1991 June 4 flare observed by OSSE [14]. From this comparison we see that there is variability in the relative energies imparted to electrons and ions during acceleration in flares, but on average they are comparable. It is important to note, however, that this sample of flares is biased as it was specifically selected because of the strong nuclear contribution. HESSI has the potential for detecting a proton capture line near 2.37 MeV that can measure the energy contained in protons below 1 MeV [31]. These low-energy protons can have other measurable effects during flares if with they are energetically important.

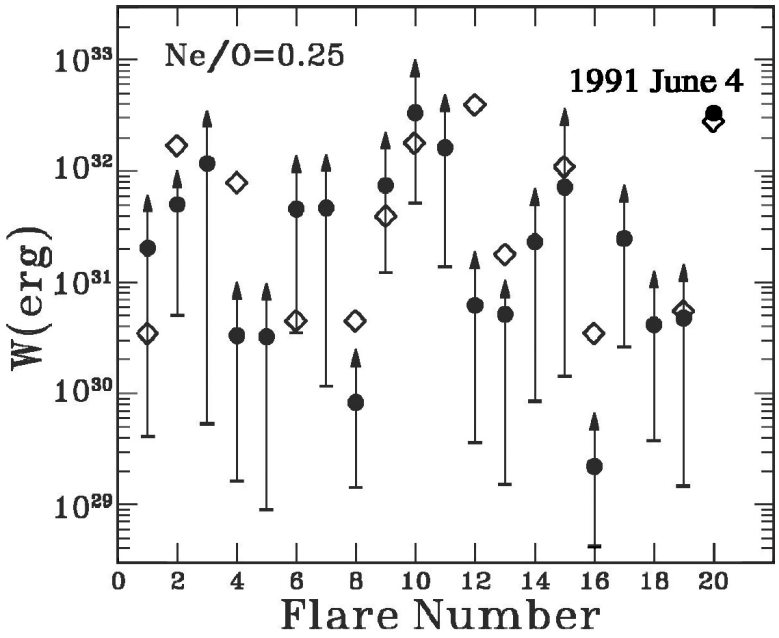


**FIGURE 7.** Calculated energy content in flare-accelerated ions (filled circles) and electrons (diamonds) [19].

## Accelerated Helium in Flares

The inset of Figure 1 shows a detail of the region containing $\alpha$-He fusion lines. We have found high fluxes in these lines relative to the de-excitation lines in the 1991 June 4 flare [14] and in the 19 *SMM* flares [32]. This led us to conclude that the accelerated $\alpha$/p ratio typically had to be large, ~0.5, for an assumed ambient $^4$He/H abundance ratio of 0.1. Mandzhavidze, *et al.* [33] suggested that the ambient ratio might also be higher in some flares and described a way in which $\gamma$-ray spectroscopy could distinguish between the two explanations. This required the measurement of other lines that only result from interactions of $\alpha$-particles on $^{56}$Fe. There is evidence for a weak line at 0.339 MeV from such interactions (inset of Figure 1) in the spectra. Based on this we concluded that, on average, the ambient $^4$He abundance is consistent

with accepted photospheric values and a high accelerated $\alpha$/p ratio is needed [34]. Mandzhavidze *et al.* performed studies of individual flares and concluded that there is evidence for both a higher accelerated $\alpha$/p ratio and enhanced ambient $^4$He [35].

These same spectral studies have provided information on the accelerated $^3$He/$^4$He ratio in flares. We studied the summed spectrum of 19 *SMM* flares in the 0.7 to 1.5 MeV region (see Figure 4). This region contains the relative strong 0.847 and 1.238 MeV lines from $^{56}$Fe, the weak line from $^{55}$Fe at 1.317 MeV, and the strong $^{24}$Mg line at 1.369 MeV. The key line features for understanding the $^3$He abundance appear near 0.937 MeV and ~1.03 MeV. The relative strength of the ~1.03 MeV feature suggests a high accelerated $\alpha$/p ratio from interactions on $^{56}$Fe and/or a high $^3$He flux producing lines after interaction with $^{16}$O. There is evidence for $^3$He in the 4 $\sigma$ detection of the 0.937 MeV line and in the shift of the ~1.03 MeV feature to higher energies in comparison with a model for $^3$He/$^4$He=0. This suggests a flare-averaged $^3$He/$^4$He ratio of ~0.1, about $10^3$ times the photospheric ratio [34,35].

## Accelerated Heavy Ions

We have revealed the broad $\gamma$-ray lines from interactions of accelerated ions with ambient H and $^4$He in spectral data from OSSE and *SMM* [36]. Lines attributable to accelerated $^{56}$Fe and $^{12}$C appear reasonably well resolved in the summed 19-flare *SMM* spectrum shown in Figure 8 after bremsstrahlung and narrow lines have been removed. The broad lines have widths of ~30% FWHM and appear to be redshifted. Broad lines from $^{24}$Mg, $^{20}$Ne, and $^{28}$Si cannot be resolved from each other and the contribution from unresolved lines. The higher energy N and O lines are also blended. Comparison of broad-line fluxes from accelerated nuclei with the respective fluxes in narrow lines from the ambient material measure relative enhancements in the accelerated particles. We find that the accelerated $^{56}$Fe abundance is enhanced over its ambient concentration by about a factor of 5 - 10, consistent with that measured in impulsive solar-energetic particles in space [37].

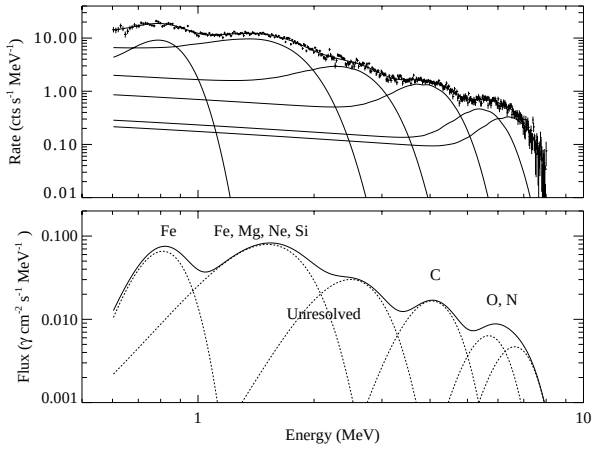


**FIGURE 8.** Gamma-ray spectrum revealing broad lines from accelerated heavy ions. a) count spectrum after subtracting narrow lines and bremsstrahlung; b) inferred photon spectrum with lines identified.

## ACKNOWLEDGMENTS

The "coming of age of solar γ-ray physics" was in large part due to the theoretical and interpretative work of Reuven Ramaty and Natalie Mandzhavidze. Regretfully, they both recently succumbed to chronic illnesses. This work was supported under NASA DPR W-18995.

## REFERENCES

1. Weekes, T. C., *Physica Scripta* **T85**, 195-209 (2000).
2. Leising, M. D., and Share, G. H., *Astrophys. J.* **357**, 638-648 (2000).
3. Diehl, R., Iyudin, A., Oberlack, U., *et al., Nucl. Phys. A* **62,** C79-C82 (1997).
4. Purcell, W. R., Grabelsky D. A., Ulmer M. P., *et al., Astrophys. J.* **413**, L85-L88 (1993).
5. Harris, M. J., Share, G. H., Messina, D.C., *Astrophys. J*. **448**, 157-163 (1995).
6. Ramaty, R., Kozlovsky, B., and Lingenfelter, R.E, *Astrophys. J. Supp*. **40**, 487-526 (1979).
7. Hunter S. D., Bertsch D. L., Catelli J. R., *et al.*, Astrophys. J. **481**, 205-240 (1997).
8. Strong A.W., Moskalenko I. V., and Reimer O., *Astrophys. J.* **537**, 763-784 (2000).
9. Falcone, A. D., *et al.*, in *AIP Conf. Proc. 528*, edited by R. A. Mewaldt, *et al.*, 2000, pp 193-196.
10. Kanbach G., Bertsch D. L., Fichtel C. E., *et al., Astron. Astrophys. Sup.* **97,** 349-353 (1993).
11. Miller, J. A., Cargill P. J., Emslie A. G., *et al.*, J. Geophys. Res. **102: (A7)**, 14631-14659 (1997).
12. Masuda, S., Kosugi, T., Hara H., *et al., Nature* **371**, 495-497 (1994).
13. Lin, R.P., *et al.*, in *High Energy Solar Physics-Anticipating HESSI*, edited by R. Ramaty and N. Mandzhavidze, San Francisco: Astron. Soc. Pacific, 2000, pp. 1-12.
14. Murphy, R. J., Share, G. H., Grove, J. E., *et al., Astrophys. J.* **490**, 883-900 (1997).
15. Ramaty, R. and Murphy, R J., *Space. Sci. Rev.* **45**, 213-268 (1987).
16. Chupp, E. L., *Science* **250,** 229-236 (1990).
17. Mandzhavidze N., and Ramaty R., *Nucl. Phys. B* **33,** 141-160 (1993).
18. Hudson H., and Ryan J., *Ann. Rev. Astron. Astr*. **33**, 239-282 (1995).
19. Ramaty, R., and Mandzhavidze, N., "Gamma Rays from Solar Flares," in *Highly Energetic Physical Processes and Mechanisms for Emission from Astrophysical Plasmas*, edited by P.C.H. Martens, S. Tsuruta, and M. A. Weber, San Francisco: Astron. Soc. Pacific, 2000, pp. 123-131.
20. Share, G.H., and Murphy, R. J., in *High Energy Solar Physics-Anticipating HESSI*, edited by R. Ramaty and N. Mandzhavidze, San Francisco: Astron. Soc. Pacific, 2000, pp. 377-386.
21. Share, G. H., and Murphy, R. J., in *AIP Conf. Proc. 528*, R. Mewaldt, *et al.*, ed., 2000, pp.181-184.
22. Murphy, R. J., *et al.*, in *AIP Conf. Proc. 280*, M. Friedlander, *et al.*, eds., 1993, pp. 619-630.
23. Harris, M. J., Share, G. H., Beall, J. H., Murphy, R. J., *Solar Physics* **142,** 171-185 (1992).
24. Feffer, P. T., *et al., Solar Physics* **171,** 419-445 (1997).
25. Hua, X.-M., and Lingenfelter, R. E., *Astrophys. J*. **319,** 555-566 (1987).
26. Yoshimori, M., Shiozawa, A., and Suga, K., *Proc. 26th Int. Cosmic Ray Conf.* **6**, 5-8 (1999).
27. Murphy, R. J., and Share, G. H., in *AIP Conf. Proc. 510*, M. McConnell and J. Ryan, eds., 2000, pp. 559-563.
28. Share, G. H., Murphy, R. J., and Skibo, J. G., in *AIP Conf. Proc. 374*, R. Ramaty, N. Mandzhavidze, X.-M. Hua, eds., 1996, pp. 162-170.
29. Share, G. H., and Murphy, R. J., *Astrophys. J.* **452**, 933-943 (1995).
30. Ramaty, R., Mandzhavidze, N., Kozlovsky, B., *et al., Astrophys. J* . **455**, L193-L196 (1995).
31. Share, G. H., Murphy, R. J., and Newton E. K., *Solar Physics*, in press.
32. Share, G. H., and Murphy, R. J., *Astrophys. J.* **485**, 409-418 (1997).
33. Mandzhavidze, N., Ramaty, R., and Kozlovksy, B. *Astrophys J*. **489**, L99-L102 (1997).
34. Share, G. H., and Murphy, R. J., *Astrophys. J.* **508**, 876-884, (1998).
35. Mandzhavidze, N., Ramaty, R., and Kozlovksy, B. *Astrophys J*. **518**, 918-925 **(**1999).
36. Share, G. H., and Murphy, R. J., *Proc. 26th Int. Cosmic Ray Conf.* **6**, 13-16 (1999).
37. Reames, D. V., *Space Sci. Rev*. **90**, 413-491 (1999).